CHEMISTRY

Triggered reversible substitution of adaptive constitutional dynamic networks dictates programmed catalytic functions

Liang Yue, Shan Wang, Itamar Willner*

The triggered substitution of networks and their resulting functions play an important mechanism in biological transformations, such as intracellular metabolic pathways and cell differentiation. We describe the triggered, cyclic, reversible intersubstitution of three nucleic acid–based constitutional dynamic networks (CDNs) and the programmed catalytic functions guided by the interconverting CDNs. The transitions between the CDNs are activated by nucleic acid strand displacement processes acting as triggers and counter triggers, leading to the adaptive substitution of the constituents and to emerging catalytic functions dictated by the compositions of the different networks. The quantitative evaluation of the compositions of the different CDNs is achieved by DNAzyme reporters and complementary electrophoresis experiments. By coupling a library of six hairpins to the interconverting CDNs, the CDN-guided, emerging, programmed activities of three different biocatalysts are demonstrated. The study has important future applications in the development of sensor systems, finite-state logic devices, and selective switchable catalytic assemblies.

INTRODUCTION

The up- and down-regulation of dynamic cellular networks by environmental physical or chemical triggers plays a major role in controlling cell viability (*1*, *2*) and occurrence of diseases (*3*), as a result of abnormal, perturbed, network pathways. Complex mechanisms participate in driving biological networks, such as signal propagation and information transfer (*4*), hierarchical control over networks (*5*), feedback (*6*) and oscillatory (*7*) mechanisms, branching and switching of reactions (*8*), and the operation of biocatalytic cascades (*9*). Several basic features lead to these unique functions of dynamic networks in nature: (i) The networks adapt themselves to environmental triggers, such as nutrients, metabolites, or biomarkers. (ii) The switchable adaptive properties of networks lead to emerging functions that control cellular processes. Substantial recent efforts are directed to the development of chemical networks guided by the principles of biological networks, a subfield of the general concept of "systems chemistry" (*10*–*12*). In these systems, complex molecular assemblies exhibit adaptive functions that are not present in the individual molecular constituents and are emerging as a result of ordered chemical ensembles. Different physical triggers, such as light (*13*), temperature (*14*), and electrical fields (*15*), and chemical triggers, such as pH (*14*), metal ions (*16*), and supramolecular H bonds (*17*), were used to control the equilibria of constitutional dynamic networks (CDNs). Beyond the adaptive properties of these networks, the use of these systems for medical applications (*3*) or the development of materials (*18*) was discussed. Within the advances in systems chemistry, peptide-based networks were used for the template-directed autocatalytic or cross-catalytic synthesis of self-replicated products (*19*, *20*), and nucleic acid templates were applied for the replication of products, using enzyme-catalyzed polymerization/nicking mechanisms (*21*). While substantial progress in developing dynamic networks has been achieved, the biomimetic systems are far from duplicating the complexity of natural networks, and the network-guided, emerging, chemical functions are unprecedented and present a future challenge in the area.

Recently, we introduced a versatile concept to apply nucleic acids as functional building blocks to construct CDNs (*22*) and demonstrated the assembly and triggered reversible reconfiguration of DNA-based CDNs with variable complexities (*23*, *24*). In these systems, we made use of several fundamental features and properties of nucleic acids: (i) Duplex structures are stabilized by complementary base pairing. The stability of duplexes can be controlled by the number of base pairs, the nature of bases, and the intercalation of ligands into duplexes. Beyond the duplexes, the base composition of nucleic acids can dictate the reconfiguration of the biopolymer into other structures, such as pH-induced i-motif and triplex structures (*25*, *26*), K^+ ion–stabilized G-quadruplexes (*27*), and ion-bridged stabilization of duplexes (e.g., T—Hg^{2+}—T or C—Ag^+—C) (*28*). (ii) Different nucleic acids can be reversibly reconfigured by auxiliary triggers (DNA switches) (*29*). For example, duplexes can be reconfigured by the strand displacement processes (*30*), different pH environments can reconfigure i-motif or triplex structures (*25*, *26*), the formation of G-quadruplexes can be switched by K^+ ions and 18-crown-6-ether (*27*), ion-stabilized complexes can be separated by appropriate ligands (*28*), and duplexes can be reversibly stabilized and destabilized by photoisomerizable intercalators (e.g., *trans*-/*cis*-azobenzene) (*31*). (iii) The base sequence of nucleic acids dictates properties that include sequence-specific recognition and binding of ligands by aptamers (*32*) and sequence-dictated DNAzymes (*33*–*35*) (e.g., cofactor-dependent phosphodiester-hydrolyzing catalysts or hemin/G-quadruplex horseradish peroxidase–mimicking DNAzyme). These unique properties were applied to develop CDNs. Different triggers, such as the separation or formation of triplexes and G-quadruplexes (*22*), and the photochemical stabilization or destabilization of duplexes (*24*) were used to stimulate the switchable reconfiguration of DNA-based CDNs. By the conjugation of DNAzyme units to the constituents, the catalytic activities of DNAzymes enabled the quantitative assessment of the compositions and dynamic transitions of CDNs. Different DNA-based CDNs were reported, and these included the triggered adaptive

Institute of Chemistry, The Hebrew University of Jerusalem, Jerusalem 91904, Israel.
*Corresponding author. Email: willnea@vms.huji.ac.il

reequilibration of [2 × 2] CDNs (*22*), the intercommunication of CDNs (*23*), and the assembly of [3 × 3] multitriggered CDNs that reveal hierarchical control over their compositions (*36*). In addition, DNA machines (e.g., tweezers) that reveal dynamic mechanical functions (*37*), and emerging catalytic functions, as a result of the operation of CDNs were demonstrated (*24*, *36*).

One important class of biological networks involves the triggered substitution of networks and their functions. For example, intracellular metabolic networks are substituted by external constraints, such as nutrient-replete or nutrient-deprived conditions (*38*). This has been demonstrated, for example, with the evolved glycolysis and oxidative phosphorylation network pathways of cells in proximity to vasculature supply of nutrients (glucose), whereas cells subjected to diminished accessibility to a vasculature supply of nutrient triggered alternative network pathways, such as the oxidation of fatty acids to support cell viability. The development of artificial interexchanging adaptive CDNs, revealing emerging functions and properties, is, however, unprecedented in the area of systems chemistry. Within our efforts to enhance the complexity of adaptive dynamic networks, we introduce the concept of "network substitution," whereby we demonstrate the guided exchange between networks, the adaptive properties of the exchanged networks, and the emergent diverse functions of the networks originating from the substitution pathways. All of these properties were not demonstrated in previous dynamic networks. The concept of network substitution is schematically outlined in Fig. 1. CDN "X," composed of four equilibrated constituents AA′, BB′, AB′, and BA′, is subjected to trigger T_1 in the presence of an auxiliary structure CC′, resulting in the substitution of components B/B′ by C/C′ to yield CDN "Y" that includes AA′, CC′, AC′, and CA′ as constituents. Applying the counter trigger T_1' on CDN "Y" restores CDN "X." Similarly, applying trigger T_2 onto CDN "X," in the presence of CC′, leads to the substitution of A/A′ by C/C′ to yield CDN "Z" consisting of constituents BB′, CC′, BC′, and CB′. Again, CDN "Z" subjected to the counter trigger T_2' restores CDN "X." Also, the treatment of CDN "Z," in the presence of AA′, with trigger T_3 results in the substitution of B/B′ by A/A′ to yield CDN "Y" composed of AA′, CC′, AC′, and CA′. The interaction of CDN "Y" with the counter trigger T_3' restores CDN "Z." Beyond adaptive cyclic and reversible transitions across three CDNs stimulated by the substitution mechanism, we demonstrate emerging catalytic functions of the CDNs where each of the interconvertible CDNs yields a different emerging catalytic function.

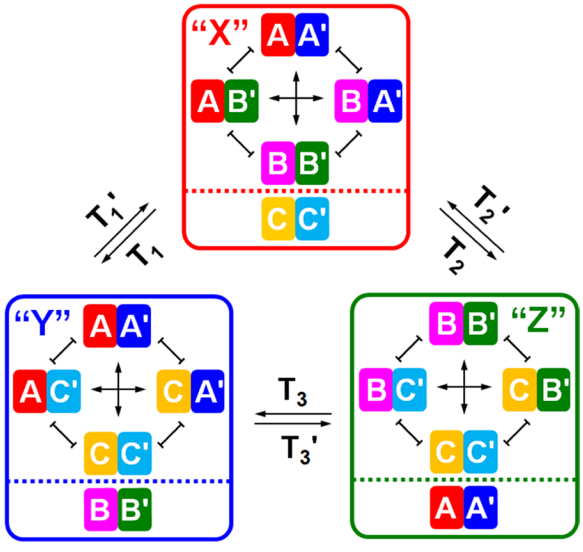

Fig. 1. Substitution mechanism. Schematic cyclic and reversible triggered intersubstitution of three CDNs. Each of the CDNs includes four different constituents and a dormant structure that does not participate in the respective equilibrated CDN. In the presence of trigger T_1, T_2, or T_3, the respective dormant structure is activated, and one of the CDN constituents is locked, resulting in the intersubstitution of one network by another CDN. By applying the appropriate counter trigger T_1', T_2', or T_3', the parent CDN is regenerated.

RESULTS

Cyclic and reversible triggered intersubstitution of three DNA-based CDNs

The principle of reversible triggered substitution between three different CDNs "X," "Y," and "Z" is shown in Fig. 2. CDN "X" includes four constituents: AA′, BB′, AB′, and BA′. In addition, the mixture includes a "dormant" structure, CC′-T_1' or CC′-T_2', where the two components C/C′ are locked by T_1' or T_2'. Although CC′-T_1' or CC′-T_2' includes the same subunits **l**/**l**′ as the constituents in CDN "X," vide infra, the locking of C/C′ by T_1' or T_2' prevents their participation in the equilibrated CDN "X." Subjecting CDN "X" to trigger T_1 leads to the unlocking of CC′-T_1' by the strand displacement (to form T_1T_1') and the concomitant hybridization of T_1 with BB′ to form the locked structure BB′-T_1, which locks B/B′ and separates AB′ and BA′ (note that T_1 is added at twofold molar concentration as compared to T_1'). Concomitantly, the unlocking of CC′-T_1' yields C/C′ that can equilibrate with A/A′ to form a new substituted CDN "Y" including AA′, CC′, AC′, and CA′. Subjecting CDN "Y" to the counter trigger T_1' displaces the locking strand T_1 associated with BB′-T_1, and concomitantly locks C/C′, in the form of CC′-T_1'. This results in the reverse transition of CDN "Y" to CDN "X." Similarly, the treatment of CDN "X" that includes the dormant structure CC′-T_2' (C/C′ is locked by T_2'), with trigger T_2 (that is complementary to T_2' and to the domains **b** and **a** associated with AA′), results in the displacement of the locking strand T_2' (to form T_2T_2' and free C/C′), and the concomitant locking of A/A′, in the form of AA′-T_2. These processes dissociate all constituents that include components A or A′ (due to the locking of AA′-T_2), resulting in the adaptive reequilibration of a new CDN "Z" comprising BB′, CC′, BC′, and CB′. Further treatment of CDN "Z" with the counter trigger T_2' leads to the regeneration of CDN "X," due to the unlocking of dormant AA′-T_2 through the formation of T_2T_2' and the concomitant depletion of C/C′ by the formation of CC′-T_2'. On the basis of the same concept, subjecting CDN "Z" that includes the dormant AA′-T_3' to trigger T_3 unlocks AA′-T_3', through the formation of T_3T_3', and locks B/B′ (BB′-T_3), leading to the triggered transition to CDN "Y." The treatment of CDN "Y" with the counter trigger T_3' restores CDN "Z" via the unlocking of BB′-T_3 and the concomitant locking of AA′-T_3'. That is, CDNs "X," "Y," and "Z" can be interconverted, in the presence of T_1/T_1', T_2/T_2', and T_3/T_3', through the unlocking and locking of appropriate structures. One major challenge in the triggered interconversion of the networks involves the appropriate structural engineering of the constituents and dormant structures in the different CDNs, to yield the thermodynamically favored transitions between the networks, guided by the appropriate triggers. (For the detailed explanation of the engineering of the constituents and the dormant structures involved in the substitution processes, see section S1 and table S1.)

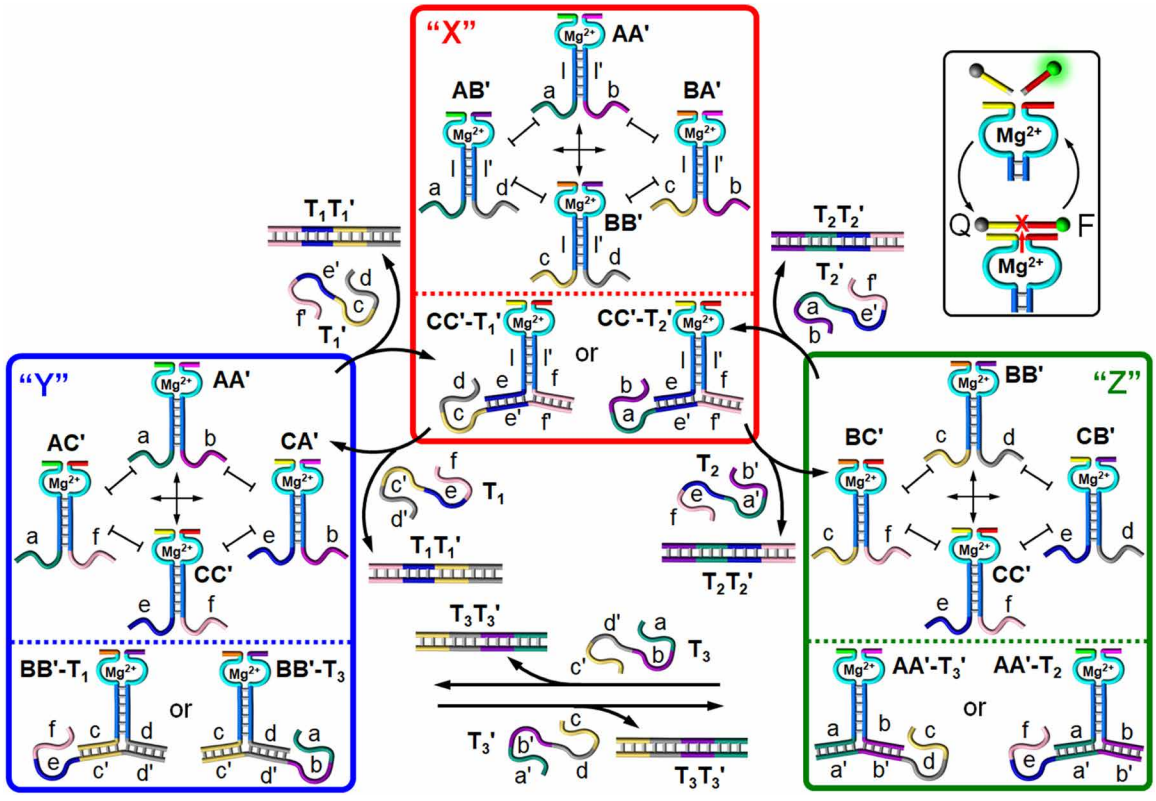

Fig. 2. Cyclic and reversible triggered intersubstitution of three DNA-based CDNs. Schematic design and mode of the operation of the cyclic and reversible triggered intersubstitution of nucleic acid–based CDNs using the strand displacement mechanism. Inset: Schematic readout of the performance of the CDNs by the application of nine different Mg^{2+} ion–dependent DNAzymes as reporter units.

Each of the constituents includes an Mg^{2+} ion–dependent DNAzyme composed of a quasi-loop/two-arm unit. The "arms" associated with different DNAzymes differ in their sequences, thus allowing the cleavage of nine different fluorophore/quencher-modified substrates. The DNAzyme units act as "reporter" elements that catalyze the cleavage of the respective substrates. The resulting time-dependent fluorescence changes provide, then, readout signals for the quantitative assessment of the constituents. By deriving appropriate calibration curves related to the catalytic activities of the constituents to their concentrations, the compositions of the different interconverted CDNs can be quantitatively evaluated. (It should be noted that structurally dictated self-assembly of DNAzyme subunits into catalytic reporters for sensing (*39*) or logic gate operations (*40*) was previously reported.)

Triggered substitution of CDN "X" by CDN "Y" and back

Figure 3A shows the time-dependent fluorescence changes generated by the reporter units linked to the constituents and the locked structure associated with CDN "X" (i), after transition to CDN "Y" using trigger T_1 (ii), and after the T_1'-induced reverse transition of CDN "Y" to CDN "X" (iii). Note that in the presence of CDN "X" (i), no catalytic activities of AC′, CA′, BC′, and CB′ are observed, since these constituents are absent in the system due to the locked CC′-T_1'. The treatment of CDN "X" with T_1 results in the transition to CDN "Y" (ii), where the time-dependent fluorescence changes were generated by AA′, CC′, AC′, and CA′ and by the locked BB′-T_1. The activities of AB′ and BA′ are almost zero in CDN "Y," since these constituents are almost fully depleted through the locking of B/B′ (to form BB′-T_1), while the activity of BB′-T_1 is, however, higher than that observed in CDN "X," due to the fact that the locking process separates AB′ and BA′ and enriches BB′-T_1 to its maximum concentration. The transition of CDN "X" to CDN "Y" triggers "ON" the activities of AC′ and CA′ and results in the lowering of the activity of CC′, as compared to that of CC′-T_1' associated with CDN "X." These results are consistent with the fact that the unlocking of CC′-T_1' and the locking of B/B′ with T_1 lead to a new equilibrated CDN "Y." Note that no catalytic activities are observed for BC′ and CB′ since these structures are not associated with CDNs "X" and "Y." The treatment of CDN "Y" with the counter trigger T_1' unlocks BB′-T_1 and locks C/C′ (to form CC′-T_1'), which restores CDN "X." This is evident by the regeneration of all catalytic activities characteristic to the constituents and the dormant structure associated with CDN "X" (iii).

The time-dependent fluorescence changes generated by variable concentrations of the respective intact constituents and the derived calibration curves relating the catalytic rates of the constituents to their concentrations are shown in fig. S1. Using these calibration curves, we quantified the concentrations of the constituents and accompanying dormant structures upon the triggered substitution of CDN "X" by CDN "Y" and back (Table 1 and fig. S2). The results indicate that in CDN "X," AA′, AB′, BA′, and BB′ are equilibrated, while CC′-T_1' is caged in a supramolecular structure that does not affect the equilibrated network. The T_1-triggered substitution of CDN "X" yields a new equilibrated CDN "Y" of AA′, AC′, CA′, and CC′, where B/B′ exist in a locked configuration, BB′-T_1, which does not affect the equilibrated CDN "Y." The triggered transition of CDN "X" to CDN "Y" and the quantitative evaluation of their compositions

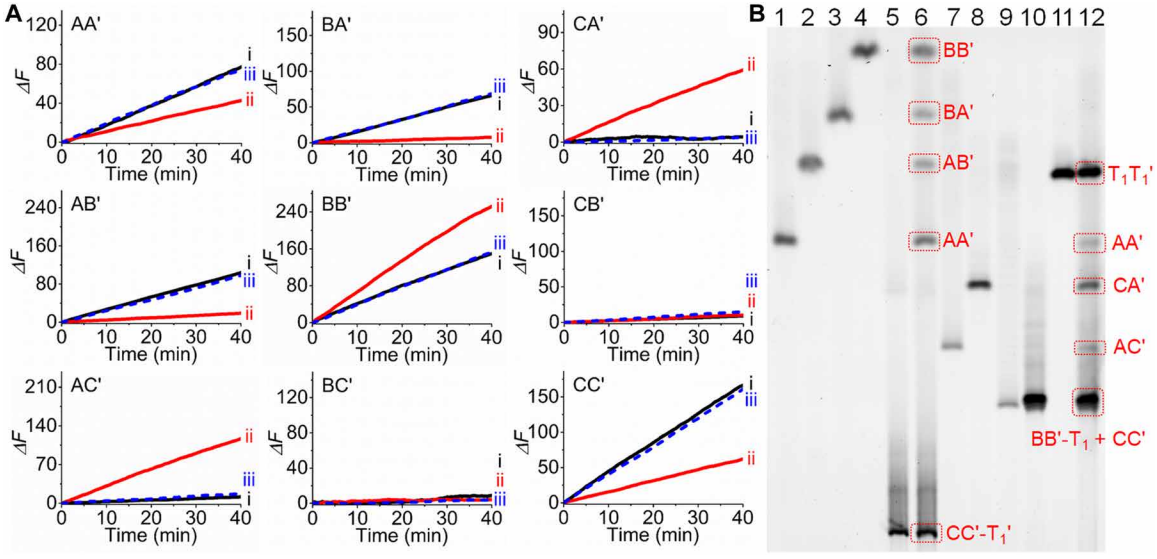

Fig. 3. Triggered substitution of CDN "X" by CDN "Y" and back. (**A**) Time-dependent fluorescence changes corresponding to the constituents and accompanying dormant structures associated with the triggered transition of CDN "X" to CDN "Y" and back: (i) before the application of any triggers; (ii) after subjecting CDN "X" to trigger T_1 and the transition to CDN "Y"; (iii) after application of the counter trigger T_1' on the resulting CDN "Y" and the recovery of CDN "X." The time-dependent fluorescence changes stimulated by the DNAzyme reporter units associated with the constituents were translated into concentrations (Table 1 and fig. S2) using the respective calibration curves (fig. S1). (**B**) Electrophoretic separation of the constituents and accompanying dormant structures associated with CDN "X" and CDN "Y" for the quantitative evaluation of the compositions of the respective CDNs.

were further supported by electrophoretic gel experiments (Fig. 3B). In lanes 1 to 5, the individual constituents AA′, AB′, BA′, and BB′ and the dormant structure CC′-T_1' are presented. Lane 6 presents the electrophoretically separated bands of CDN "X" and the accompanying CC′-T_1'. In lanes 7 to 11, the individual structures AC′, CA′, CC′, BB′-T_1, and T_1T_1' are presented. Lane 12 shows the separated bands corresponding to CDN "Y," generated by the T_1-stimulated substitution of CDN "X." Using the ImageJ software and comparing the intensities of the separated bands to the intensities of the individual structures at known concentrations (1 μM), we evaluated the compositions of CDNs (Table 1, in brackets). The results demonstrate the T_1-guided interconversion of CDN "X" to CDN "Y." The compositions of CDNs "X" and "Y" evaluated by the respective DNAzymes agree well with those derived by the electrophoretic experiment.

Triggered substitution of CDN "X" by CDN "Z" and back

The same set of experiments was applied for the T_2-induced substitution of CDN "X" by CDN "Z" and for the reverse equilibration of CDN "Z" into CDN "X" using the counter trigger T_2' (cf. Fig. 2). Figure S3A shows the time-dependent fluorescence changes generated by the constituents and the dormant structure associated with CDN "X" (i) after the T_2-induced transition to CDN "Z" (ii) and after subjecting CDN "Z" to T_2' and the recovery of CDN "X" (iii). Locking of A/A′ in AA′-T_2 depletes AB′ and BA′ (almost no catalytic activities) and increases the activity of AA′ due to the accumulation of all A/A′ (from the separated AB′ and BA′), and the equilibration of the remaining B/B′ with the unlocked C/C′ (from CC′-T_2') leads to the formation of CDN "Z" composed of BB′, CC′, BC′, and CB′ (ii). Note that in CDN "Z," the constituents AC′ and CA′ are nonexistent. The treatment of CDN "Z" with T_2' restores CDN "X," and the activities associated with CDN "X" are fully regenerated (iii). Using appropriate calibration curves (fig. S1), we evaluated the compositions of the different CDNs (Table 1 and fig. S3B). Further quantitative evaluation of the contents of the constituents was obtained by electrophoretic experiments (fig. S3C and accompanying discussion), and the results are shown in Table 1 (in brackets). Very good agreements of the compositions of the CDNs evaluated by the DNAzyme activities and by the electrophoretic separation exist.

Triggered substitution of CDN "Z" by CDN "Y" and back

In addition, we examined the transition of CDN "Z" to CDN "Y" and back (cf. Fig. 2). Figure S4A shows the time-dependent fluorescence changes generated by the constituents and accompanying dormant structure associated with CDN "Z" (i) after the T_3-induced transition to CDN "Y" (ii) and after the recovery of CDN "Z" by the subsequent addition of T_3' (iii). Using the appropriate calibration curves (fig. S1), we evaluated the contents of the constituents and accompanying dormant structures (Table 1 and fig. S4B). In addition, we performed quantitative electrophoretic analysis of the compositions of different CDNs, and the results are presented in fig. S4C with a detailed discussion. The electrophoretically evaluated compositions (Table 1, in brackets) are in good agreement with the values derived from the activities of DNAzyme reporters. The results demonstrate the T_3-induced transition of CDN "Z" to CDN "Y" and the reverse transition of CDN "Y" to CDN "Z" using T_3'.

All the above results demonstrate the cyclic and reversible transitions between CDNs "X," "Y," and "Z" using a substitution pathway that applies the strand displacement mechanism and T_1/T_1', T_2/T_2', and T_3/T_3' as driving fuels. It is noteworthy, however, that besides the triggered interconversion across networks, the composition of each network can be controlled by internal triggers that regulate the internal equilibration of the network (figs. S5 to S7 and accompanying discussion).

Table 1. Concentrations of the equilibrated constituents in the different CDN systems. (i) CDN "X" before the addition of T_1. (ii) CDN "Y" generated by the addition of T_1 to CDN "X." (iii) CDN "X" before the addition of T_2. (iv) After subjecting CDN "X" to T_2 and the transition to CDN "Y." (v) CDN "Z" before the interaction with T_3. (vi) After the addition of T_3 and the T_3-triggered substitution of CDN "Z" by CDN "Y."

System	Concentration (μM)								
	[AA′]	[AB′]	[AC′]	[BA′]	[BB′]	[BC′]	[CA′]	[CB′]	[CC′]
Substitution of CDN "X" by CDN "Y"									
(i)*	0.64	0.41	0.05	0.41	0.57	0.06	0.01	0.04	0.98
(i)†	(0.62)	(0.37)	(—)‡	(0.36)	(0.61)	(—)‡	(—)‡	(—)‡	(0.99)
(ii)*	0.34	0.06	0.65	0.03	0.99	0.01	0.6	0.05	0.37
(ii)†	(0.31)	(—)‡	(0.64)	(—)‡	(—)§	(—)‡	(0.61)	(—)‡	(—)§
Substitution of CDN "X" by CDN "Z"									
(iii)*	0.61	0.38	0.05	0.38	0.58	0.02	0.01	0.06	1.00
(iii)†	(0.63)	(0.41)	(—)‡	(0.45)	(0.59)	(—)‡	(—)‡	(—)‡	(0.95)
(iv)*	0.98	0.06	0.01	0.04	0.46	0.51	0.05	0.53	0.47
(iv)†	(0.97)	(—)‡	(—)‡	(—)‡	(0.45)	(0.47)	(—)‡	(0.52)	(0.52)
Substitution of CDN "Z" by CDN "Y"									
(v)*	0.99	0.01	0.05	0.04	0.49	0.53	0.02	0.56	0.46
(v)†	(1.04)	(—)‡	(—)‡	(—)‡	(0.47)	(0.56)	(—)‡	(0.54)	(0.51)
(vi)*	0.32	0.06	0.68	0.03	0.98	0.05	0.64	0.03	0.32
(vi)†	(0.29)	(—)‡	(0.68)	(—)‡	(—)§	(—)‡	(0.66)	(—)‡	(—)§

*Data provided by the catalytic activities of the respective DNAzyme reporter units and appropriate calibration curves. †Data provided by the electrophoretic separation of the constituent mixtures and the quantitative analysis of the separated stained bands (for details, see the Supplementary Materials). ‡No detectable bands. §Bands cannot be evaluated due to the overlap.

Emerging catalytic functions guided by the interconverting CDNs

An important outcome of the study is, however, the emergence of three different switchable catalytic functions driven by the intersubstitution of the three CDNs (Fig. 4). CDNs "X," "Y," and "Z" were subjected to a mixture of six hairpins H_1 to H_6. In the presence of CDN "X," AB′ and BA′ select hairpins H_1 and H_2, respectively, as substrates. The cleaved-off fragments $H_{1\text{-}1}$ and $H_{2\text{-}2}$ self-assemble into the emerging supramolecular catalytic Mg^{2+} ion–dependent DNAzyme (DNAzyme **1**). The cleavage of the fluorophore/quencher-modified substrate S_1 by DNAzyme **1** leads to the fluorescence of the substrate fragment $S_{1\text{-}1}$, which provides the readout signal for the catalytic process. Treatment of CDN "X" with T_1 results in the substitution of CDN "X" by CDN "Y." The resulting AC′ and CA′ in CDN "Y" select and cleave hairpins H_3 and H_4, respectively, from the "hairpin pool," and the cleaved-off fragments $H_{3\text{-}1}$ and $H_{4\text{-}2}$ self-assemble, in the presence of K^+ ions and hemin, into the hemin/G-quadruplex horseradish peroxidase–mimicking DNAzyme, DNAzyme **2**. DNAzyme **2** catalyzes the oxidation of Amplex Red by H_2O_2 to yield the fluorescent product Resorufin as the readout signal for the emerging catalytic function of CDN "Y." The treatment of CDN "Y" with the counter trigger T_1' restores CDN "X." This reverse process switches "OFF" DNAzyme **2** and reactivates DNAzyme **1**. In addition, substitution of CDN "X," in the presence of T_2, yields CDN "Z." The constituents BC′ and CB′ associated with CDN "Z" select and cleave H_5 and H_6 to yield the fragmented $H_{5\text{-}2}$ and $H_{6\text{-}1}$. The auxiliary strand P that includes a single-stranded loop conjugated to two hairpin domains is unlocked by $H_{5\text{-}2}$ and $H_{6\text{-}1}$ to yield the supramolecular Pb^{2+} ion–dependent DNAzyme, DNAzyme **3**. The cleavage of the fluorophore/quencher-modified substrate S_2 by DNAzyme **3** leads to the fluorescent fragment $S_{2\text{-}1}$ as the readout signal for the emerging catalytic function of CDN "Z." The treatment of CDN "Z" with the counter trigger T_2' restores CDN "X," which switches "OFF" DNAzyme **3** and switches "ON" DNAzyme **1**. Alternatively, subjecting CDN "Z" to T_3 leads to the substitution of CDN "Z" with CDN "Y," resulting in the switching-off of DNAzyme **3** and the switching-on of DNAzyme **2**. That is, the cyclic and reversible interconversion of three CDNs by means of the triggered substitution mechanism leads to the cyclic control over switchable, emerging, catalytic functions dictated by the CDNs. (For further detailed clarification of the CDN-guided assembly of the DNAzymes, see fig. S8 and accompanying discussion.)

Figure 5A (panel I) shows the catalytic activities of DNAzyme **1** in CDN "X" before (i) and after (ii) the T_1-induced transition to CDN "Y" and after the regeneration of CDN "X" using T_1' (iii). The transition of CDN "X" to CDN "Y" switches "OFF" DNAzyme **1**, and its activity is recovered after the reverse transition of CDN "Y" to CDN "X." Figure 5A (panel II) depicts the activities of DNAzyme **1** in CDN "X" (i) after the T_2-triggered transition to CDN "Z" (ii) and after the T_2'-stimulated regeneration of CDN "X" (iii). The activities of DNAzyme **1** can be switched "OFF"/"ON" by the triggered substitution of CDN "X" by CDN "Z" and back. For comparison, Fig. 5A (panel III) shows no activities of DNAzyme **1** upon the T_3-induced transition of CDN "Z" to CDN "Y" and back in the presence of T_3'. Evidently, DNAzyme **1** is switched "OFF" in CDNs "Z" and "Y." Figure 5B (panel IV) demonstrates no activities of DNAzyme **2** in CDN "X" (i). After the T_1-induced transition to CDN "Y," DNAzyme **2** is switched on (ii), and after the reverse T_1'-stimulated transition of CDN "Y" to CDN "X," DNAzyme **2** is switched off again (iii). Figure 5B (panel V) shows no activities of DNAzyme **2** upon the triggered substitution of CDN "X" by CDN "Z" and back. These results are consistent with the fact that CDNs "X" and "Z" do not

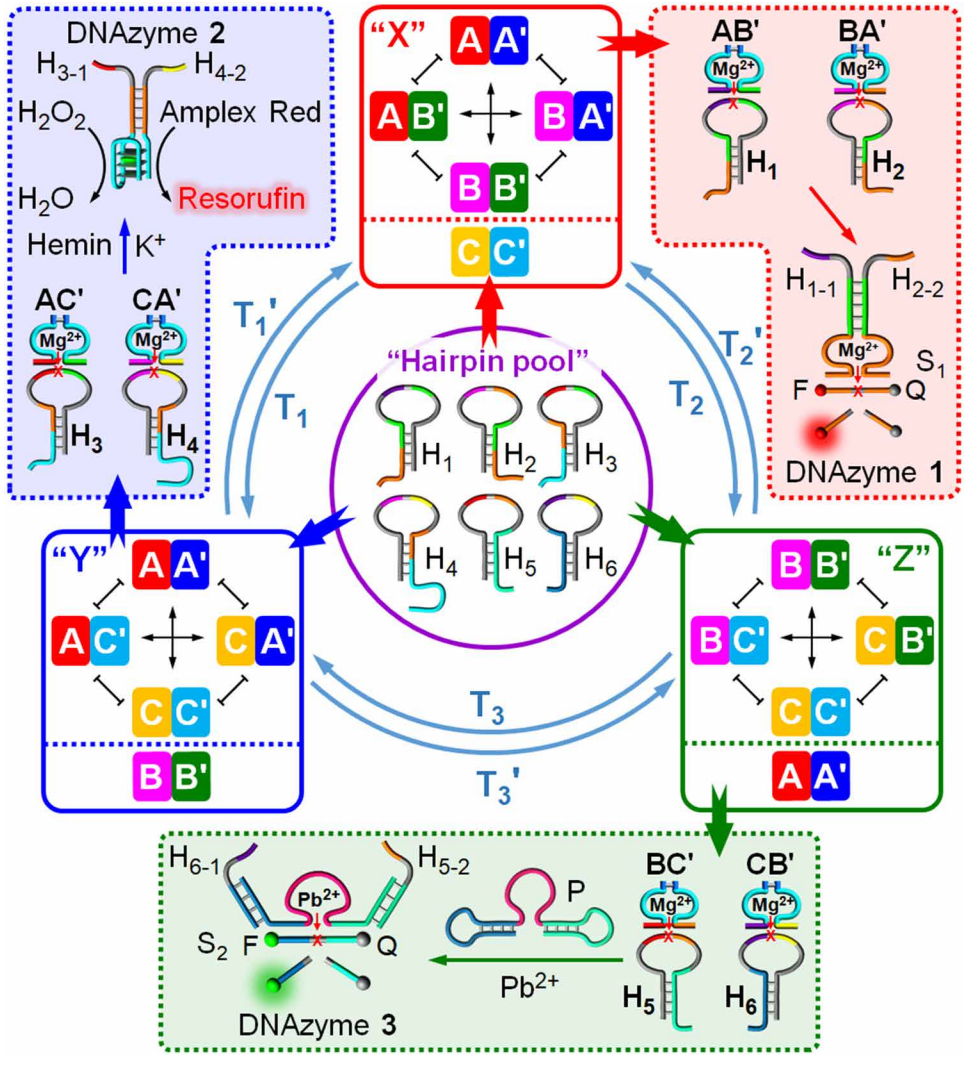

Fig. 4. Emerging catalytic functions guided by the interconverting CDNs. Programmed cyclic and reversible catalytic functions triggered by the intersubstituted CDNs. The three interexchangeable CDNs are subjected to a set of hairpin substrates H_1 to H_6. Each of the triggered, intersubstituted CDNs selects selectively the respective hairpin substrates from the hairpin pool, resulting in the guided formation of the respective catalytic DNAzymes. CDN "X" cleaves hairpins H_1 and H_2 to yield DNAzyme **1** (Mg^{2+} ion–dependent DNAzyme). CDN "Y" cleaves hairpins H_3 and H_4 to yield DNAzyme **2** (hemin/G-quadruplex DNAzyme). CDN "Z" cleaves hairpins H_5 and H_6, and the cleaved products self-assemble, in the presence of the added strand P, into DNAzyme **3** (Pb^{2+} ion–dependent DNAzyme).

lead to the formation of DNAzyme **2**. The activities of DNAzyme **2** upon the T_3-induced transition of CDN "Z" to CDN "Y" and back using the counter trigger T_3' are shown in Fig. 5B (panel VI). The activity of DNAzyme **2** is switched on upon transition of CDN "Z" to CDN "Y" and, subsequently, is switched off upon the regeneration of CDN "Z." Last, the reversible substitution-triggered transitions between CDNs "X," "Y," and "Z" to switch the activities of DNAzyme **3** were explored (cf. Fig. 4). Figure 5C (panel VII) shows no catalytic activities of DNAzyme **3** either in CDN "X" or CDN "Z," implying that DNAzyme **3** is not generated by these CDNs. Figure 5C (panel VIII) depicts the activities of DNAzyme **3** in CDN "X" (i) after the T_2-triggered substitution of CDN "X" by CDN "Z" (ii) and after the T_2'-stimulated regeneration of CDN "X" (iii). The activity of DNAzyme **3** is switched on by the transition of CDN "X" to CDN "Z" and is switched off by the regeneration of CDN "X." Figure 5C (panel IX) demonstrates the activities of DNAzyme **3** in the presence of CDN "Z" (i) after its substitution by CDN "Y" using T_3 (ii) and upon the subsequent T_3'-stimulated reequilibration of CDN "Z" (iii). The results reveal that the triggered substitution of CDN "Z" leads to the selective activation of DNAzyme **3**. Overall, the set of results presented in Fig. 5 and fig. S9 demonstrates that the cyclic and reversible intersubstitution across CDNs "X," "Y," and "Z" leads to triggered emerging functions of DNAzyme **1**, DNAzyme **2**, or DNAzyme **3**.

DISCUSSION

The study has addressed a major element of complexity associated with the development of artificial nucleic acid–based CDNs mimicking biological systems, namely, the triggered substitution and interconversion of networks. We have constructed three networks—"X," "Y," and "Z"—and demonstrated the triggered, cyclic, and reversible interconversion across three CDNs. The transitions between the networks were stimulated by the unlocking and locking of appropriate

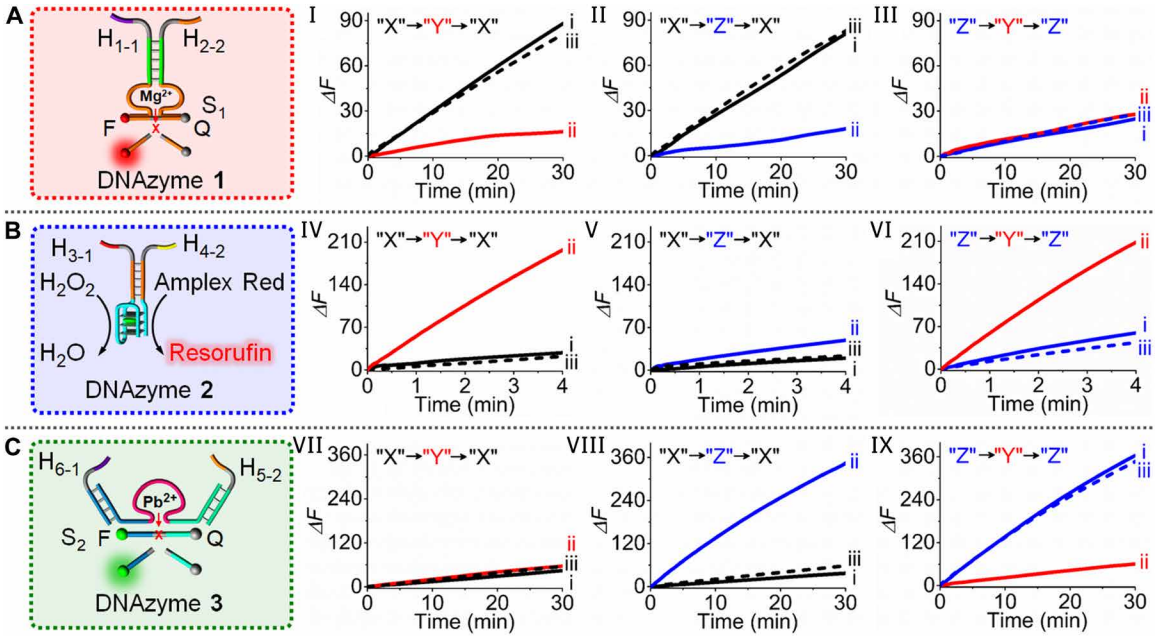

Fig. 5. Catalytic activities of the emerging DNAzymes. (**A** to **C**) Time-dependent fluorescence changes corresponding to the emerging catalytic functions: (A) DNAzyme **1**, (B) DNAzyme **2**, and (C) DNAzyme **3**, upon the cyclic and reversible triggered intersubstitution between CDNs "X," "Y," and "Z." Panels I, IV, and VII show the transition of CDN "X" to CDN "Y" and back: (i) CDN "X" before the addition of trigger T_1; (ii) after subjecting CDN "X" to T_1 and the transition to CDN "Y"; (iii) after applying the counter trigger T_1' to the resulting CDN "Y" and the reequilibration of CDN "X." Panels II, V, and VIII show the substitution of CDN "X" by CDN "Z" and back: (i) CDN "X" before the addition of trigger T_2; (ii) after the treatment of CDN "X" with T_2 and the equilibration of CDN "Z"; (iii) after subjecting the resulting CDN "Z" to the counter trigger T_2' and the reequilibration of CDN "X." Panels III, VI, and IX show the transition of CDNs "Z" to "Y" and back: (i) CDN "Z" before the application of trigger T_3; (ii) after the T_3-induced transition of CDN "Z" to CDN "Y"; (iii) after applying the counter trigger T_3' to the resulting CDN "Y" and the regeneration of CDN "Z."

structures using the strand displacement process in the presence of nucleic acid triggers or counter triggers, leading to the exchange of the constituents and to the formation of substituted CDNs. We demonstrated that by coupling of the interconverting CDNs to a library of hairpins, the interconverting CDNs guided the formation of three different programmed catalysts. The emergence of switchable catalytic functions by the intersubstitution of the CDNs mimics complex biological pathways and adds new dimensions to systems chemistry. Beyond the significance of the systems in mimicking natural networks, these systems can be applied as sensors, logic gates, and finite-state devices and as functional assemblies for switchable, programmed catalysis.

MATERIALS AND METHODS

Materials

Hepes, magnesium chloride, potassium chloride, hemin, Amplex Red, hydrogen peroxide, and lead(II) acetate trihydrate were purchased from Sigma-Aldrich. DNA oligonucleotides were purchased from Integrated DNA Technologies Inc. (Coralville, IA). "GelRed nucleic acid gel stain" was purchased from Invitrogen. Ultrapure water from NANOpure Diamond (Barnstead) source was used in all of the experiments.

The oligonucleic acid sequences used in the study include the following: (**1**) A, 5′-TCTGTTCAGCGAT CAAACTCTTACAACCAACGAAGCAACCA-3′; (**2**) B, 5′-TGTCCTCAGCGATCAAA CTCTTACAACATGCAATGCCAGAA-3′; (**3**) C, 5′-TCCATTCAGCGATCAAACTCT TACAACAACAAGTACAACAAGAA-3′; (**4**) A′, 5′-ACCGTAGACGACCGAAGTAA GAGTTTGCACCCATGTTCCTGAT-3′; (**5**) B′, 5′-ACGTACACCATCTCGAAAGTAA GAGTTTGCACCCATGTTTCAGTT-3′; (**6**) C′, 5′-ACACAGTCACAGTCACAAGTAA GAGTTTGCACCCATGTTTAGCTT-3′; (**7**) T_1, 5′-ACACAGTCACAGTCACAACAAC AAGTACAACAAGAATTCTGGCATTG CATGTTTCGAGATGGTGTACGT-3′; (**8**) T_1', 5′-ACGTACACCATCTCGAAACATGCAATGCCAGAATTCTTGTTGTACTTGT TGTTGTGACTGTGACTGTGT-3′; (**9**) T_2, 5′-ACACAGTCACAGTCACAACAACAAG TACAACAAGAATGGTTGCTTCGTTGGTTCGGTCGTCTACGGT-3′; (**10**) T_2', 5′-ACCGTAGACGACCGAACCAACGAAGCAACCATTCTTGTTGTACTTGTTGTTGTGA CTGTGACTGTGT-3′; (**11**) T_3, 5′-TTCTGGCATTGCATGTTTCGAGATGGTGTACGT ACCGTAGACGACCGAACCAACGAAGCAACCA-3′; (**12**) T_3', 5′-TGGTTGCTTCGT TGGTTCGGTCGTCTACGGTACGTACACCATCTCGAAACATGCAATGCCAGAA-3′; (**13**) $T_{aa'}$, 5′-CTTCGTTGGTAATCGGTCGTC-3′; (**14**) $T_{bb'}$, 5′-CATTGCATGTAATT CGAGATGG-3′; (**15**) $T_{cc'}$: 5′-GTACTTGTTGTAAGACTGTGACT-3′; (**16**) $T_{ab'}$: 5′-CTT CGTTGGTAATTCGAGATGG-3′; (**17**) $T_{ac'}$, 5′-CTTCGTTGGTAAGACTGTGACT-3′; (**18**) $T_{cb'}$: 5′-GTACTTGTTGTAATTCGAGATGG-3′; (**19**) sub1 (AA′), 5′-Cy5.5-TCAGG AT**rA**GGAACAG-IBRQ-3′; (**20**) sub2 (AB′), 5′-FAM-ACTGAAT**rA**GGAACAG-BHQ1-3′; (**21**) sub3 (AC′), 5′-Cy5-AGCTAAT**rA**GGAACAG-BHQ2-3′; (**22**) sub4 (BA′), 5′-ROX-TCAGGAT**rA**GGAG BHQ2-3′; (**24**) sub6 (BC′), 5′-Cy5.5-AGCTAAT**rA**GGAGGACIBRQ-3′; (**25**) sub7 (CA′), 5′-ROX-TCAGGAT**rA**GGAATGGBHQ2-3′; (**26**) sub8 (CB′), 5′-ROX-ACT GAAT**rA**GGAATGGBHQ2-3′; (**27**) sub9 (CC′), 5′-FAM-AGCTAAT**rA**GGAATGG-BHQ1-3′; (**28**) sub1-noFQ (AA′), 5′-TCAGGAT**rA**GGAACAG-3′; (**29**)

sub2-noFQ (AB′), 5′-ACTGAAT**rA**GGAACAG-3′; (**30**) sub3-noFQ (AC′), 5′-AGCTAAT**rA**GGAACAG-3′; (**31**) sub4-noFQ (BA′), 5′-TCAGGAT**rA**GGAGGAC-3′; (**32**) sub5-noFQ (BB′), 5′-ACTG AAT**rA**GGAGGAC-3′; (**33**) sub6-noFQ (BC′), 5′-AGCTAAT**rA**G-GAGGAC-3′; (**34**) sub7-noFQ (CA′), 5′-TCAGGAT**rA**GGAATGG-3′; (**35**) sub8-noFQ (CB′), 5′-ACTGAA T**rA**GGAATGG-3′; (**36**) sub9-noFQ (CC′), 5′-AGCTAAT**rA**GGAATGG-3′; (**37**) H_1, 5′-C TGCTCA-GCGATGTTCTTCTTGCAACTGAAT**rA**GGAACAGATATACA GAACATCG-3′; (**38**) H_2, 5′-GGTGGTTCTAAATAATCAGGA-T**rA**GGAGGACAGCAAGAAGAA CCACCCATGTTACTCT-3′; (**39**) H_3, 5′-GAGGGATAGTGACTTCAAGCTAAT**rA**GG AACAG-ACATCACACTATCCC-3′; (**40**) H_4, 5′-CCCTTAGTGTTAATAT-CAGGAT**rA** GGAATGGAGAAGTCACTAAGGGAGGGAGG-3′; (**41**) H_5, 5′-AAATGACGTAAAT AAGCTAAT**rA**GGAGGA-CAATAATCGTCATTTGGT-3′; (**42**) H_6, 5′-ACGAATCTGC TCTCTAAACTGAAT**rA**GGAATGGATAATAAGCAGATT-3′; (**43**) P, 5′-GAGAGCAGATTCGAACTGCTCTCCGAGCCGGTC-GAAATCGTCAATCC AAATGACGATT-3′; (**44**) S_1 (for DNAzyme **1**), 5′-Cy5-AGAGTAT**rA**GGAGCA-BHQ2-3′; (**45**) S_2 (for DNA-zyme **3**), 5′-ROX-TGACGAT**rA**GGAGCAG-BHQ2-3′; (**46**) A_m, 5′-TCTGTTCAG CGATCAAACTCTTACAACCAACGAAG-CAACCAAAAAAAAAAAAAAAAAA-3′; (**47**) B_m, 5′-TGTCCT-CAGCGATCAAACTCTTACAACATGCAATGCCAGAAAAA AAAAAAAAAAAAAA-3′; (**48**) C_m, 5′-TCCATTCAGCGAT-CAAACTCTTACAACA ACAAGTACAACAAGAAAAAAAAAA AAAAAAAAAAAAAAA-3′; (**49**) A'_m, 5′-AAAAAAAAAAAAC-CGTAGACGACCGAAGTAAGAGTTTGCACCCATGTTCCTG AT-3′; (**50**) B'_m, 5′-AAAAAAAACGTACACCATCTCGAAAG-TAAGAGTTTGCACCC ATGTTTCAGTT-3′; (**51**) C'_m, 5′-AAAAA-AAAAAAAAAAAAAAAAAAAACACA GTCACAGTCA-CAAGTAAGAGTTTGCACCCATGTTTAGCTT-3′.

The ribonucleobase cleavage site, **rA**, in the substrates is indicated in bold, and the respective DNAzyme sequences are underlined.

Characterizations

Fluorescence spectra were recorded with a Cary Eclipse Fluorometer (Varian Inc.). The polyacrylamide gel electrophoresis (PAGE) gels were run on a Hoefer SE 600 electrophoresis unit. The excitation of FAM, ROX, Cy5, Cy5.5, and Resorufin were performed at 496, 588, 648, 685, and 570 nm, respectively. The emission of FAM, ROX, Cy5, Cy5.5, and Resorufin were recorded at 516, 608, 668, 706, and 585 nm, respectively.

Methods

Preparation of the CDNs and the cyclic reversible transitions between the CDNs

The transition of CDNs "X" to "Y" and back is taken as an example. CDN "X" that includes the constituents AA′, AB′, BA′, and BB′ and the dormant structure CC′-T_1′ was prepared as follows. A mixture of A (**1**), B (**2**), C (**3**), A′ (**4**), B′ (**5**), C′ (**6**), and T_1′ (**8**), 1 μM each, in 10 mM Hepes buffer (pH 7.2), which includes 20 mM $MgCl_2$, was annealed at 85°C, cooled down to 25°C at a rate of 0.33°C min^{-1}, and allowed to equilibrate for 2 hours at 25°C to yield CDN "X," which includes the constituents AA′, AB′, BA′, and BB′ and the locked structure CC′-T_1′. The prepared CDN "X" was subjected to trigger T_1 (**7**), 2 μM, and allowed to equilibrate at 28°C for 12 hours to yield CDN "Y," which consists of the constituents AA′, AC′, CA′, and CC′ and the locked BB′-T_1. The resulting CDN "Y" was treated with the counter trigger T_1′ (**8**), 2 μM, and allowed to equilibrate at 28°C for an additional time interval of 12 hours to regenerate CDN "X."

Probing cyclic and reversible triggered transitions between CDNs "X," "Y," and "Z"

The transition of CDN "X" to CDN "Y" and back is described as an example. For evaluating the contents of the constituents AA′, AB′, and BA′, aliquots of 60 μl were withdrawn from the equilibrated CDNs and treated with sub1 (**19**), sub2 (**20**), sub4 (**22**), sub3-noFQ (**30**), sub5-noFQ (**32**), sub6-noFQ (**33**), sub7-noFQ (**34**), sub8-noFQ (**35**), and sub9-noFQ (**36**), 3 μl of 100 μM each. To evaluate the contents of the constituents AC′, CA′, and CC′, aliquots of 60 μl were withdrawn from the equilibrated CDNs and treated with sub3 (**21**), sub7 (**25**), sub9 (**27**), sub1-noFQ (**28**), sub2-noFQ (**29**), sub4-noFQ (**31**), sub5-noFQ (**32**), sub6-noFQ (**33**), and sub8-noFQ (**35**), 3 μl of 100 μM each. For probing the contents of the constituents BB′, BC′, and CB′, aliquots of 60 μl were withdrawn from the equilibrated CDNs and treated with sub5 (**23**), sub6 (**24**), sub8 (**26**), sub1-noFQ (**28**), sub2-noFQ (**29**), sub3-noFQ (**30**), sub4-noFQ (**31**), sub7-noFQ (**34**), and sub9-noFQ (**36**), 3 μl of 100 μM each. Subsequently, the time-dependent fluorescence changes generated from the cleavage of the different substrates by the respective catalytic constituents were followed. Using the appropriate calibration curves corresponding to the rates of cleavage of the different substrates by variable concentrations of the intact constituents (see fig. S1), the contents of the constituents in the different CDNs were evaluated.

Preparation of hairpins H_1, H_2, H_3, H_4, H_5, H_6, and P

Taking H_1 as an example, H_1 (**37**), 50 μM, in 10 mM Hepes buffer (pH 7.2), which includes 20 mM $MgCl_2$, was annealed at 95°C, cooled down quickly to 25°C, and allowed to equilibrate for 2 hours at 25°C.

Preparation of samples for the emerging catalytic functions

The different equilibrated interconverting CDNs were prepared by the cyclic and reversible transitions between CDNs "X," "Y," and "Z," 300 μl each. Then, each of the CDNs was treated with the mixture of hairpins H_1, H_2, H_3, H_4, H_5, and H_6, 6 μl of 50 μM each, 15 μl of 2 M KCl, and 3 μl of 100 μM hemin, and incubated at 28°C for 8 hours.

Probing the catalytic activities of the emerging Mg^{2+} ion–dependent DNAzyme (DNAzyme 1) in the different CDNs

Aliquots of 30 μl were withdrawn from the each incubated mixture and treated with substrate S_1 (**44**), 3 μl of 100 μM, and 30 μl of 10 mM Hepes buffer (pH 7.2), which included 20 mM $MgCl_2$. Subsequently, the time-dependent fluorescence changes generated from the cleavage of S_1 by DNAzyme **1** in the different CDNs were followed.

Probing the catalytic activities of the emerging hemin/G-quadruplex DNAzyme (DNAzyme 2) in the different CDNs

For the oxidation of Amplex Red, of 4-μl aliquots of each incubated mixture, Amplex Red (0.85 μl of 6 mM), and H_2O_2 (3.5 μl of 25 mM) were added to 56 μl of 10 mM Hepes buffer (pH 7.2), which included 20 mM $MgCl_2$ and 100 mM KCl. Subsequently, the time-dependent fluorescence changes generated from the oxidation of Amplex Red by DNAzyme **2** in the different CDNs were recorded at λ_{em} = 585 nm.

Probing the catalytic activities of the emerging Pb^{2+} ion–dependent DNAzyme (DNAzyme 3) in the different CDNs

Aliquots of 20 μl of the each incubated mixture were treated with P (**43**), 1 μl of 20 μM, and incubated at 28°C for 10 min. Aliquots of

10 μl of the resulting incubated mixtures, $Pb(Ac)_2$ (10 μl of 1 μM), and substrate S_2 (**45**) (3 μl of 100 μM) were added to 40 μl of 10 mM Hepes buffer (pH 7.2), which included 20 mM $MgCl_2$. Subsequently, the time-dependent fluorescence changes upon the cleavage of S_2 by DNAzyme **3** in the different CDNs were followed.

Quantitative evaluation of the contents of the constituents in the different CDNs by PAGE gel electrophoresis

Native PAGE gel electrophoresis experiments were performed using a polyacrylamide gel (12%, acrylamide/bisacrylamide 19:1), gel thickness of 1 mm. Mixtures were separated upon applying a 150-V potential, 10°C (to eliminate the dissociation of duplexes). The separations were conducted for time intervals of 40 hours (for the transition of CDN "X" to CDN "Y") and 30 hours (for the transition of CDN "X" to CDN "Z" and the transition of CDN "Z" to CDN "Y").

The transition of CDN "X" to CDN "Y" is taken as an example. The mixtures of the constituents corresponding to CDN "X" and CDN "Y" generated by the treatment of CDN "X" with T_1 were loaded as duplicates in the gel. Note that to enhance the separation, some of the constituents were modified with conjugated tethers, which do not participate in the stabilization/destabilization of the constituents (A_m instead of A, A_m' instead of A′, C_m instead of C, and C_m' instead of C′). The intact individual structures AA′, AB′, BA′, BB′, AC′, CA′, CC′, CC′-T_1', BB′-T_1, and T_1T_1' at identical concentrations (1 μM) were loaded as references in predefined lanes. The PAGE gel was stained with GelRed, and the intensities of the separated bands corresponding to CDN "X" and CDN "Y" were quantitatively analyzed by ImageJ software upon comparing the intensities of the respective separated bands of the CDNs to the intensities developed by the respective individual references with known concentrations.

In the transition of CDN "X" to CDN "Z," B_m instead of B, B_m' instead of B′, C_m instead of C, and C_m' instead of C′ were used to improve the separation of the constituents. In the transition of CDN "Z" to CDN "Y," A_m instead of A, A_m' instead of A′, C_m instead of C, and C_m' instead of C′ were used to improve the separation of the constituents.

SUPPLEMENTARY MATERIALS

Supplementary material for this article is available at http://advances.sciencemag.org/cgi/content/full/5/5/eaav5564/DC1

Section S1. Guiding rules for the assembly of the CDNs for the triggered interconversion of the CDNs

Fig. S1. Calibration curves.

Fig. S2. Concentration changes following the transition of CDN "X" to CDN "Y" and back.

Fig. S3. Results of the triggered substitution of CDN "X" by CDN "Z" and back.

Fig. S4. Results of the triggered substitution of CDN "Z" by CDN "Y" and back.

Fig. S5. Internal equilibration of CDN "X".

Fig. S6. Internal equilibration of CDN "Y".

Fig. S7. Internal equilibration of CDN "Z".

Fig. S8. Detailed design of the emerging catalytic functions.

Fig. S9. Catalytic rates of the emerging DNAzymes guided by the intersubstituted CDNs.

Table S1. NUPACK-predicted and experimental concentrations of the constituents and dormant structures associated with CDN "X" and CDN "Y".

REFERENCES AND NOTES

1. R. Jaenisch, A. Bird, Epigenetic regulation of gene expression: How the genome integrates intrinsic and environmental signals. *Nat. Genet.* **33**, 245–254 (2003).
2. C. Vogel, E. M. Marcotte, Insights into the regulation of protein abundance from proteomic and transcriptomic analyses. *Nat. Rev. Genet.* **13**, 227–232 (2012).
3. A.-L. Barabási, N. Gulbahce, J. Loscalzo, Network medicine: A network-based approach to human disease. *Nat. Rev. Genet.* **12**, 56–68 (2011).
4. A. Ma'ayan, S. L. Jenkins, S. Neves, A. Hasseldine, E. Grace, B. Dubin-Thaler, N. J. Eungdamrong, G. Weng, P. T. Ram, J. J. Rice, A. Kershenbaum, G. A. Stolovitzky, R. D. Blitzer, R. Iyengar, Formation of regulatory patterns during signal propagation in a mammalian cellular network. *Science* **309**, 1078–1083 (2005).
5. M. Levine, E. H. Davidson, Gene regulatory networks for development. *Proc. Natl. Acad. Sci. U.S.A.* **102**, 4936–4942 (2005).
6. D. Angeli, J. E. Ferrell Jr., E. D. Sontag, Detection of multistability, bifurcations, and hysteresis in a large class of biological positive-feedback systems. *Proc. Natl. Acad. Sci. U.S.A.* **101**, 1822–1827 (2004).
7. M. R. Atkinson, M. A. Savageau, J. T. Myers, A. J. Ninfa, Development of genetic circuitry exhibiting toggle switch or oscillatory behavior in *Escherichia coli*. *Cell* **113**, 597–607 (2003).
8. U. S. Bhalla, P. T. Ram, R. Iyengar, MAP kinase phosphatase as a locus of flexibility in a mitogen-activated protein kinase signaling network. *Science* **297**, 1018–1023 (2002).
9. W. Weber, M. Fussenegger, Engineering of synthetic mammalian gene networks. *Chem. Biol.* **16**, 287–297 (2009).
10. R. F. Ludlow, S. Otto, Systems chemistry. *Chem. Soc. Rev.* **37**, 101–108 (2008).
11. E. Mattia, S. Otto, Supramolecular systems chemistry. *Nat. Nanotechnol.* **10**, 111–119 (2015).
12. G. Ashkenasy, T. M. Hermans, S. Otto, A. F. Taylor, Systems chemistry. *Chem. Soc. Rev.* **46**, 2543–2554 (2017).
13. L. A. Ingerman, M. L. Waters, Photoswitchable dynamic combinatorial libraries: Coupling azobenzene photoisomerization with hydrazone exchange. *J. Org. Chem.* **74**, 111–117 (2009).
14. N. Giuseppone, J.-M. Lehn, Protonic and temperature modulation of constituent expression by component selection in a dynamic combinatorial library of imines. *Chem. A Eur. J.* **12**, 1715–1722 (2006).
15. N. Giuseppone, J.-M. Lehn, Electric-field modulation of component exchange in constitutional dynamic liquid crystals. *Angew. Chem. Int. Ed.* **45**, 4619–4624 (2006).
16. P. Kovaříček, J.-M. Lehn, Merging constitutional and motional covalent dynamics in reversible imine formation and exchange processes. *J. Am. Chem. Soc.* **134**, 9446–9455 (2012).
17. V. Berl, I. Huc, J.-M. Lehn, A. DeCian, J. Fischer, Induced fit selection of a barbiturate receptor from a dynamic structural and conformational/configurational library. *Eur. J. Org. Chem.* **1999**, 3089–3094 (1999).
18. Y. Bai, A. Chotera, O. Taran, C. Liang, G. Ashkenasy, D. G. Lynn, Achieving biopolymer synergy in systems chemistry. *Chem. Soc. Rev.* **47**, 5444–5456 (2018).
19. D. H. Lee, K. Severin, Y. Yokobayashi, M. R. Ghadiri, Emergence of symbiosis in peptide self-replication through a hypercyclic network. *Nature* **390**, 591–594 (1997).
20. G. Ashkenasy, R. Jagasia, M. Yadav, M. R. Ghadiri, Design of a directed molecular network. *Proc. Natl. Acad. Sci. U.S.A.* **101**, 10872–10877 (2004).
21. A. Padirac, T. Fujii, A. Estévez-Torres, Y. Rondelez, Spatial waves in synthetic biochemical networks. *J. Am. Chem. Soc.* **135**, 14586–14592 (2013).
22. S. Wang, L. Yue, Z. Shpilt, A. Cecconello, J. S. Kahn, J.-M. Lehn, I. Willner, Controlling the catalytic functions of DNAzymes within constitutional dynamic networks of DNA nanostructures. *J. Am. Chem. Soc.* **139**, 9662–9671 (2017).
23. L. Yue, S. Wang, S. Lilienthal, V. Wulf, F. Remacle, R. D. Levine, I. Willner, Intercommunication of DNA-based constitutional dynamic networks. *J. Am. Chem. Soc.* **140**, 8721–8731 (2018).
24. S. Wang, L. Yue, Z.-Y. Li, J. Zhang, H. Tian, I. Willner, Light-induced reversible reconfiguration of DNA-based constitutional dynamic networks: Application to switchable catalysis. *Angew. Chem. Int. Ed.* **57**, 8105–8109 (2018).
25. K. Gehring, J.-L. Leroy, M. Guéron, A tetrameric DNA structure with protonated cytosine-cytosine base pairs. *Nature* **363**, 561–565 (1993).
26. Y. Hu, A. Cecconello, A. Idili, F. Ricci, I. Willner, Triplex DNA nanostructures: From basic properties to applications. *Angew. Chem. Int. Ed.* **56**, 15210–15233 (2017).
27. C.-H. Lu, X.-J. Qi, R. Orbach, H.-H. Yang, I. Mironi-Harpaz, D. Seliktar, I. Willner, Switchable catalytic acrylamide hydrogels cross-linked by hemin/G-quadruplexes. *Nano Lett.* **13**, 1298–1302 (2013).
28. Y. Miyake, H. Togashi, M. Tashiro, H. Yamaguchi, S. Oda, M. Kudo, Y. Tanaka, Y. Kondo, R. Sawa, T. Fujimoto, T. Machinami, A. Ono, Mercury^{II}-mediated formation of thymine–Hg^{II}–thymine base pairs in DNA duplexes. *J. Am. Chem. Soc.* **128**, 2172–2173 (2006).
29. F. Wang, X. Liu, I. Willner, DNA switches: From principles to applications. *Angew. Chem. Int. Ed.* **54**, 1098–1129 (2015).
30. D. Y. Zhang, G. Seelig, Dynamic DNA nanotechnology using strand-displacement reactions. *Nat. Chem.* **3**, 103–113 (2011).
31. Y. Kamiya, H. Asanuma, Light-driven DNA nanomachine with a photoresponsive molecular engine. *Acc. Chem. Res.* **47**, 1663–1672 (2014).
32. S. E. Osborne, I. Matsumura, A. D. Ellington, Aptamers as therapeutic and diagnostic reagents: Problems and prospects. *Curr. Opin. Chem. Biol.* **1**, 5–9 (1997).

33. R. R. Breaker, G. F. Joyce, A DNA enzyme that cleaves RNA. *Chem. Biol.* **1**, 223–229 (1994).
34. G. F. Joyce, Forty years of in vitro evolution. *Angew. Chem. Int. Ed.* **46**, 6420–6436 (2007).
35. P. Travascio, Y. Li, D. Sen, DNA-enhanced peroxidase activity of a DNA-aptamer-hemin complex. *Chem. Biol.* **5**, 505–517 (1998).
36. Z. Zhou, L. Yue, S. Wang, J.-M. Lehn, I. Willner, DNA-based multi-constituent dynamic networks: Hierarchical adaptive control over the composition and cooperative catalytic functions of the systems. *J. Am. Chem. Soc.* **140**, 12077–12089 (2018).
37. L. Yue, S. Wang, A. Cecconello, J.-M. Lehn, I. Willner, Orthogonal operation of constitutional dynamic networks consisting of DNA-tweezer machines. *ACS Nano* **11**, 12027–12036 (2017).
38. R. J. DeBerardinis, N. S. Chandel, Fundamentals of cancer metabolism. *Sci. Adv.* **2**, e1600200 (2016).
39. D. M. Kolpashchikov, A binary deoxyribozyme for nucleic acid analysis. *Chembiochem* **8**, 2039–2042 (2007).
40. R. Pei, E. Matamoros, M. Liu, D. Stefanovic, M. N. Stojanovic, Training a molecular automaton to play a game. *Nat. Nanotechnol.* **5**, 773–777 (2010).

Acknowledgments

Funding: This research was supported by the Israel Science Foundation (ISF) and the Minerva Center for Biohybrid Complex Systems. **Author contributions:** L.Y., S.W., and I.W. designed the systems and participated in writing the paper. L.Y. and S.W. performed the experiments and analyzed the results. **Competing interests:** The authors declare that they have no competing interests. **Data and materials availability:** All data needed to evaluate the conclusions in the paper are present in the paper and/or the Supplementary Materials. Additional data related to this paper may be requested from the corresponding author according to the material transfer agreement.

Submitted 27 September 2018
Accepted 26 March 2019
Published 10 May 2019
10.1126/sciadv.aav5564

Citation: L. Yue, S. Wang, I. Willner, Triggered reversible substitution of adaptive constitutional dynamic networks dictates programmed catalytic functions. *Sci. Adv.* **5**, eaav5564 (2019).

Science Advances

Triggered reversible substitution of adaptive constitutional dynamic networks dictates programmed catalytic functions

Liang Yue, Shan Wang and Itamar Willner

Sci Adv **5** (5), eaav5564.
DOI: 10.1126/sciadv.aav5564